Published in final edited form as:
Obesity (Silver Spring). 2008 October ; 16(10): 2379–2387. doi:10.1038/oby.2008.350.

Brief Genetic Analysis:

Effects of Ritonavir on Adipocyte Gene Expression: Evidence for a Stress-Related Response

Diane C. Adler-Wailes, **Evan L. Guiney**, **Jashin Koo**, and **Jack A. Yanovski**
From the Unit on Growth and Obesity, Developmental Endocrinology Branch, NICHD, National Institutes of Health, DHHS

Abstract

To understand the molecular mechanisms underlying the development of dyslipidemia and lipodystrophy that occurs after administration of aspartic acid protease inhibitors, we examined transcriptional profiles using cDNA microarrays in 3T3-L1 adipocytes exposed for 2 - 21 days to 10 μM ritonavir. The expression levels of ~12,000 transcripts were assessed using the MgU74Av2 mouse microarray chip. Ritonavir altered gene expression of inflammatory cytokines, stress response genes localized to endoplasmic reticulum, oxidative stress genes, apoptosis related genes, and expression of genes involved in cell adhesion and extracellular matrix remodeling. Microarray analysis also identified a novel gene down-regulated by ritonavir, Cidea, whose expression levels may affect free fatty acid metabolism. These changes suggest a unique, stress-related pattern in adipocytes induced by chronic exposure to the protease inhibitor, ritonavir.

Introduction

The mechanisms underlying the pathogenesis of human immunodeficiency virus associated lipodystrophy syndrome are not well understood, but involve redistribution of adipose tissue as well as metabolic abnormalities in adipocyte function (1). Highly active antiretroviral therapy that includes protease inhibitors has been associated with peripheral lipoatrophy (2) and visceral adiposity (3), and protease inhibitor mediated lipoatrophy has been proposed to be due to alterations in adipocyte differentiation and lipolysis (4).

Two previous short-term investigations have employed microarray approaches in 3T3-L1 adipocytes to identify potential candidate genes whose expression might explain the development of protease inhibitor-mediated lipodystrophy syndrome (5,6). However, longer term effects of protease inhibitors on gene expression have not been examined. We hypothesized that protease inhibitor-induced lipodystrophy syndrome involves coordinated cumulative changes in adipocyte gene expression that would indicate stress-related cellular activation. We therefore examined changes in gene expression in 3T3-L1 adipocytes treated chronically with the protease inhibitor, ritonavir.

Results and Discussion

Gene expression was compared by microarray between control and 10 μM ritonavir-treated 3T3-L1 cells at 2, 6, 10, 14, and 21 days after initiation of differentiation. Tables 1A, 1B, and 1C show fold changes in gene expression throughout the 21 days of ritonavir exposure. There was no effect of ritonavir treatment on genes required for the adipocyte phenotype that are

Please address correspondence to: Jack A. Yanovski, M.D., Ph.D., Head, Unit on Growth and Obesity, National Institutes of Health, 10 Center Drive, Hatfield Clinical Research Center, Room 1E-3330, MSC 1103, Bethesda, Maryland 20892-1103, Phone: 301-496-0858; Fax: 301-402-0574; E-mail: jy15i@nih.gov.

expressed early in differentiation, confirming previously reported findings (7). While there was a small but significant decrease in C/EBPα expression at 6 and 10 days ($p<0.01$, $p<0.05$), respectively, by 14 and 21 days the expression was equivalent to vehicle (Figure 1A). PPARγ gene expression was unchanged at all time points (Figure 1B) which agrees with previous reports (8). None of the other adipocyte-specific differentiation genes examined were significantly altered by ritonavir treatment (Table 1A). There were no significant differences in expression of genes relevant for insulin signaling (Table 1A).

Cellular stress in adipocytes is often accompanied by the onset of inflammation, endoplasmic reticulum and oxidative stress, which is then followed by physical damage to adipocytes and surrounding endothelial cells (9,10). We observed an expression pattern of inflammation induced by ritonavir different from that found in obesity (11). Typically, in obesity, inflammation is characterized by increased secretion of TNFα and leptin as well as decreased secretion of adiponectin by adipocytes leading to infiltration of macrophages (11). While we were not able to examine changes in TNFα by real time PCR due to low expression in these 3T3-L1 adipocytes, leptin gene expression was unchanged (Table 1B). Adiponectin gene expression was significantly reduced with short term (2d) and chronic (14 and 21d) exposure to ritonavir ($p<0.02$, Figure 1E), a finding consistent with increased oxidative stress (12). Our results agree with Lagathu, et al who demonstrated that acute treatment of fully differentiated human adipocytes with 10 μM ritonavir resulted in increased ROS production and decreased adiponectin protein expression (13). Further, ritonavir treatment significantly increased expression of interleukin 9 ($p<0.0007$) but not interleukin 6 ($p=0.22$), chemokine ligand 9 ($p<0.0002$), and tumor necrosis factor receptor family, member 1b (p75; $p<0.02$) with the largest increases at 14 and 21 days (Table 1B,Figure 2A). Our results differ from those of Vernochet, et al., who reported significant inductions from 5 days' exposure to 10 μM ritonavir in TNFα and IL-6 expression in cultured human adipocytes (14) and from Grigem, et al. who reported that short-term ritonavir exposure increased TNFα receptor expression in a dose dependent manner (8), probably because of the different cells and time course examined.

Endoplasmic reticulum (ER) stress has been implicated as a response to metabolic stress (15). One metabolic stress reported in protease inhibitor treated adipocytes is excess basal free fatty acid release (16-18). We observed a trend towards an increase ($p=0.073$) in activating transcription factor 3 (Atf 3), a significant increase in Atf4 ($p<0.0008$) expression, and a significant decrease ($p<0.0003$) in phosphoenolpyruvate carboxykinase (Pck1) expression (Tables 1A and 1B). Reverse transcriptase real time PCR (RT-PCR) for Atf3 and Pck1 showed the largest increase ($p<0.01$) in Atf3 expression at 14 days (Figure 2B) and the largest decrease ($p<0.01$) in Pck1 expression at 10 days (Figure 1C). Parker, et al. also showed a significant increase in Atf3 gene expression by RT-PCR in 3T3-L1 adipocytes treated with ritonavir for 16-24 hours, and a significant decrease in Pck1 gene expression with 24 hour exposure to 30 μM lopinavir or 10 μM nelfinavir (6). Atf3 activation has been suggested to be a cellular response to stress through which cells attempt to prevent JNK-induced apoptosis, because it induces the anti-apoptotic factor, heat shock protein 27 (19). Pck1 is believed to be a key enzyme for glyceroneogenesis. Decreased Pck1 expression has also been observed in metabolic syndrome and correlated with excess free fatty acid release (20). Further, flavin containing monooxygenase (FMO1) expression was significantly decreased ($p<0.0001$, Table 1B). This decrease is another ER insult, in that yeast FMO1 activity is important in maintaining the ER oxidative state necessary for folding proteins containing disulfide bonds (21). Interestingly, in rat primary hepatocytes, ritonavir treatment induced apoptosis through activating the unfolded protein response in ER (22) where FMO1 is localized. Other genes induced in expression during ER stress include CHOP and an active splice variant of XBP-1 (23,24). There were no differences in CHOP-10 expression or total XBP-1 expression by microarray analysis during ritonavir treatment (Table 1B). We examined the splicing pattern of XBP-1 at 14 and 21 days, which were the time points where other stress markers were significantly changed (Figures 1D

& E and 2A, C, & D). There were no significant differences (14 day: $p<0.82$, 21 day: $p<0.69$) in the ratio of spliced XBP-1 transcript to unspliced XBP-1 transcript in ritonavir- vs. vehicle-treated cells at 14 days (0.163±0.014 vs. 0.173±0.015) and 21 days (0.124±0.041 vs. 0.149 ±0.047), respectively. Therefore, in 3T3-L1 adipocytes, ritonavir treatment did not induce expression of genes known to initiate the unfolded protein response in ER (24,25).

Microarray analysis suggested that ritonavir treated adipocytes may have oxidative stress, because cytochrome C oxidase, subunit VIa, polypeptide 2 (Cox6a2) expression was significantly increased ($p<0.0005$; Table 1B). These data are consistent with the observed increase in MAP kinase-interacting serine/threonine kinase 2 (Mknk2; $p<0.013$) and Bcl2-associated X protein (Bax) expression ($p<0.0315$; Table 1B). Cox6a2, Mknk2, and Bax expression were confirmed by RT-PCR, with Mknk2 showing increases at 2, 6, and 21 days, preceding increased Cox6a2 expression at 14 and 21 days, and Bax induction at 21 days (Figure 1D and Figure 2C & D). These changes, collectively, suggest a cytokine induced stress response (26,27) which could lead to apoptosis or necrosis (28). Indeed, endothelial cells treated with 15 μM ritonavir produced 32% more superoxide anion and had increased permeability when compared to controls (29). In addition, ritonavir treatment of human endothelial cells induced cytotoxicity and subsequent necrosis through mitochondrial damage (30). Further, treatment of human adipocytes with 20 μM ritonavir induced apoptosis (31).

Changes in the extracellular matrix may also contribute to the susceptibility of adipocytes to invasion/apoptosis (32,33). Microarray analysis revealed decreased expression of many genes involved in cell adhesion such as: latent transforming growth factor beta binding protein 1 (Ltbp1, $p<0.028$) which was confirmed by RT-PCR ($p<0.01$ at 21 days, Figure 2E), transforming growth factor, beta induced ($p<0.019$), microfibrillar associated protein 5 ($p<0.0034$), dermatopontin ($p<0.0001$), integrin alpha 6 ($p<0.0002$), and tissue inhibitor metalloproteinase 3 (Timp 3, $p<0.0003$; Table 1C). Ltbp1 is important for association of a cytokine, TGF-β with the extracellular matrix, and lower expression of Ltbp1 might result in increased TGF-β signaling (34). Timp3 is also involved in remodeling of extracellular matrix, and decreased expression by ritonavir (Table 1C) would result in increased matrix metalloproteinase (MMP) activity. Indeed, ritonavir treatment of 3T3-L1 cells reversed the decrease in MMP-9 activity normally seen during adipogenesis (35).

Lastly, gene profiling demonstrated significantly lower ($p<0.0093$, Table 1B, Figure 2F) cell death-inducing DNA fragmentation factor, alpha subunit-like effector A (Cidea) in ritonavir treated 3T3-L1 cells. This finding has not been previously reported. Cidea expression in 293T cells induced apoptosis by a caspase independent mechanism (36), but perhaps more importantly, low Cidea expression has been shown to be related to increased basal lipolysis in both human and mouse adipocytes (37,38). Although free fatty acid release was not measured in these studies, we and others have previously shown increased basal free fatty acid release in 3T3-L1 adipocytes chronically treated with 10 μM ritonavir (16) or acutely treated with nelfinavir in doses between 5-40 μM (17).

Gene profiling in 3T3-L1 cells chronically exposed to ritonavir has revealed a unique pattern of adipocyte response that includes distinct effects on inflammatory mediators, ER and oxidative stress, and potential remodeling of extracellular matrix proteins which may predispose adipocytes to apoptosis. Future studies confirming these findings should be carried out using other protease inhibitors such as atazanavir that may have a more favorable metabolic profile.

Experimental Methods

Cell Culture and Protease Inhibitor Treatment

Murine 3T3-L1 cells (ATCC; Manassas, VA) were grown on Corning/Costar dishes (Corning, NY) in a 5% CO_2 atmosphere at 37°C and maintained in Dulbecco's Modified Eagle's medium (DMEM, 4500 mg glucose/liter) supplemented with 10% fetal bovine serum, 2 mM glutamine, 8 μg/ml biotin, 110 μg/ml pyruvate, 100 units/ml penicillin, and 100 μg/ml streptomycin. Confluent cells were differentiated by addition of 10^{-6} M dexamethasone, 0.5 mM isobutylmethylxanthine, and 5 μg/ml insulin to DMEM medium with 10% fetal bovine serum for 3 days, with medium changed once every 24 hours. Cells receiving ritonavir were given differentiation medium containing a final concentration of 10 μM ritonavir dissolved in 0.1% ethanol as previously described (16) in both differentiation cocktail and DMEM maintenance medium as specified below. Purified ritonavir was graciously provided by Abbot Laboratories under a materials transfer agreement. Control cells were given 0.1% ethanol (vehicle) containing medium without ritonavir. After 3 days, the differentiation medium was withdrawn, and cells were maintained in DMEM with 10% FBS plus either vehicle or 10 μM ritonavir for a total of 21 days, with addition of fresh medium every 24 hours.

Microarray Analysis

Cells were harvested at 2, 6, 10, 14, and 21 days for total RNA using Trizol reagent (Invitrogen; Carlsbad, CA). Equivalent amounts of total RNA from six 10 cm dishes (treated identically) were pooled, and poly A RNA was then purified with Ambion poly A purest kit (Ambion; Austin, TX) from the pooled RNA sample. One poly A RNA sample treated with either vehicle or ritonavir from each time point was hybridized to Affymetrix (Santa Clara, CA) MgU74Av2 gene expression arrays. The time course experiment, poly A RNA purification, and hybridization to Affymetrix MgU74Av2 gene expression arrays was repeated a second time.

Real Time PCR

Total RNA samples (as described above) were DNase treated (Invitrogen), purified by phenol/chloroform/isoamyl alcohol (Invitrogen) extraction, and precipitated with 70% ethanol. Concentration and integrity of DNase treated RNA was determined with an Agilent (Santa Clara, CA) 2100 bioanalyzer. Approximately 250 ng of RNA was reversed transcribed using the Superscript III Platinum Two-Step qRT-PCR kit (Invitrogen) to make cDNA template used for real time PCR reactions. Applied Biosystems (Foster City, CA) TaqMan fluorescent assays were used to determine relative mRNA expression for each gene studied. To examine the effect of ritonavir on relative mRNA expression, expression ratios were calculated taking into account the efficiency of the PCR reaction for both reference and target genes. The reference gene for all analyses was 18s ribosomal RNA.

Semi-quantitative PCR for XBP-1 Transcripts

cDNA templates were diluted (1:5) in PCR hot start mix (SuperArray Biosciences, Frederick, MD). For amplification of unspliced (U-XBP1) and spliced (S- XBP1) transcripts, a single pair of primers was used: sense; GAA CCA GGA GTT AAG AAC ACG and antisense; AGG CAA CAG TGT CAG AGT CC (Invitrogen, Carlsbad, CA) as previously described (39). PCR conditions: 95°C for 15min followed by 40 cycles of 95°C for 30sec, 60°C for 30sec, and 72° C for 30sec (40). PCR products were electrophoresed on 4-12% gradient tris borate EDTA (TBE) polyacrylamide gels (Invitrogen, Carlsbad, CA). Presence of S-XBP1 was confirmed by both amplification of spliced variant with sequence specific primers (40), and by comparison to positive control samples generously provided by Brian D. Dynlacht (New York University School of Medicine, NYU Cancer Institute). TBE gels were stained with 0.5 μg/ml ethidium

bromide followed by quantitation of U-XBP1 and S-XBP1 bands using ImageQuant software (GE Healthcare, Piscataway, NJ).

Statistical Analysis

Intensities from the microarray hybridization were calculated using Affymetrix ArraySuite (Version 4) from the individual experiments and quality control of the two experiments was assessed using a model based analysis (41). Change call and expression data for each gene from the two replicates were compared for consistency between experiments. A correlation coefficient was calculated from log transformed expression indices (for each time point within treatment) and ranged between 0.88-0.91. Since both experiments were consistent with respect to the change call comparisons and direction of trends, intensities for those genes called present were averaged across both experiments. A linear regression model was developed to examine the effect of ritonavir on gene expression over time with the following equation:

$$y_{ijk}=m+Trt_i+\mathrm{Time}_j+(Trt x \mathrm{Time})_{ij}+e_{ijk}$$

The overall mean is *m*, and the other terms denote deviation from the mean due to treatment effect ($Trt_{i)}$, time effect ($Time_J$), treatment by time interaction ($(Trt \times Time)_{ij}$), and error (e_{ijk}). Transcripts were tested for significance at the $p<0.05$ level for treatment, time, or treatment by time interaction. Fold changes in gene expression due to ritonavir treatment are reported for each time point with the p value for Trt_i in Tables 1A, 1B, and 1C. Additional data (adjusted intensities from microarray hybridization with 95% confidence limits) are included separately as an appendix.

For confirmation of gene expression with real time PCR, mean within time ratios from both microarray experiments were calculated for each time point comparing relative expression of ritonavir treated cells to vehicle (42). The mean within time ratios averaged across the 2 experiments were compared to a hypothesized mean=1, and were considered significantly different from 1 at $p<0.05$. All means are reported with standard errors. The ratio of S-XBP1 to U-XBP1 was calculated, and subjected to arcsine-square root transformation before analysis using unpaired t-tests. Non-transformed means with SEM's are reported in the text.

Supplementary Material

Refer to Web version on PubMed Central for supplementary material.

Acknowledgements

This research was supported by the Intramural Research Program of the NIH, grant Z01-HD-000641 from the National Institute of Child Health and Human Development, National Institutes of Health (to JAY).

References

1. Koutkia P, Grinspoon S. HIV-associated lipodystrophy: pathogenesis, prognosis, treatment, and controversies. Annu Rev Med 2004;55:303–17. [PubMed: 14746523]
2. Villarroya F, Domingo P, Giralt M. Lipodystrophy associated with highly active anti-retroviral therapy for HIV infection: the adipocyte as a target of anti-retroviral-induced mitochondrial toxicity. Trends Pharmacol Sci 2005;26:88–93. [PubMed: 15681026]
3. Miller KD, Jones E, Yanovski JA, Shankar R, Feuerstein I, Falloon J. Visceral abdominal-fat accumulation associated with use of indinavir. Lancet 1998;351:871–5. [PubMed: 9525365]
4. Rudich A, Ben-Romano R, Etzion S, Bashan N. Cellular mechanisms of insulin resistance, lipodystrophy and atherosclerosis induced by HIV protease inhibitors. Acta Physiol Scand 2005;183:75–88. [PubMed: 15654921]

5. Pacenti M, Barzon L, Favaretto F, et al. Microarray analysis during adipogenesis identifies new genes altered by antiretroviral drugs. Aids 2006;20:1691–705. [PubMed: 16931933]
6. Parker RA, Flint OP, Mulvey R, et al. Endoplasmic reticulum stress links dyslipidemia to inhibition of proteasome activity and glucose transport by HIV protease inhibitors. Mol Pharmacol 2005;67:1909–19. [PubMed: 15755908]
7. Dowell P, Flexner C, Kwiterovich PO, Lane MD. Suppression of preadipocyte differentiation and promotion of adipocyte death by HIV protease inhibitors. J Biol Chem. 2000
8. Grigem S, Fischer-Posovszky P, Debatin KM, Loizon E, Vidal H, Wabitsch M. The effect of the HIV protease inhibitor ritonavir on proliferation, differentiation, lipogenesis, gene expression and apoptosis of human preadipocytes and adipocytes. Horm Metab Res 2005;37:602–9. [PubMed: 16278782]
9. Nakatani Y, Kaneto H, Kawamori D, et al. Involvement of endoplasmic reticulum stress in insulin resistance and diabetes. J Biol Chem 2005;280:847–51. [PubMed: 15509553]
10. Wellen KE, Hotamisligil GS. Inflammation, stress, and diabetes. J Clin Invest 2005;115:1111–9. [PubMed: 15864338]
11. Wellen KE, Hotamisligil GS. Obesity-induced inflammatory changes in adipose tissue. J Clin Invest 2003;112:1785–8. [PubMed: 14679172]
12. Hattori Y, Akimoto K, Gross SS, Hattori S, Kasai K. Angiotensin-II-induced oxidative stress elicits hypoadiponectinaemia in rats. Diabetologia 2005;48:1066–74. [PubMed: 15864528]
13. Lagathu C, Eustace B, Prot M, et al. Some HIV antiretrovirals increase oxidative stress and alter chemokine, cytokine or adiponectin production in human adipocytes and macrophages. Antivir Ther 2007;12:489–500. [PubMed: 17668557]
14. Vernochet C, Azoulay S, Duval D, et al. Human immunodeficiency virus protease inhibitors accumulate into cultured human adipocytes and alter expression of adipocytokines. J Biol Chem 2005;280:2238–43. [PubMed: 15525648]
15. Hotamisligil GS. Role of endoplasmic reticulum stress and c-Jun NH2-terminal kinase pathways in inflammation and origin of obesity and diabetes. Diabetes 2005;54(Suppl 2):S73–8. [PubMed: 16306344]
16. Adler-Wailes DC, Liu H, Ahmad F, et al. Effects of the human immunodeficiency virus-protease inhibitor, ritonavir, on basal and catecholamine-stimulated lipolysis. J Clin Endocrinol Metab 2005;90:3251–61. [PubMed: 15741249]
17. Rudich A, Vanounou S, Riesenberg K, et al. The HIV protease inhibitor nelfinavir induces insulin resistance and increases basal lipolysis in 3T3-L1 adipocytes. Diabetes 2001;50:1425–31. [PubMed: 11375344]
18. Kovsan J, Ben-Romano R, Souza SC, Greenberg AS, Rudich A. Regulation of adipocyte lipolysis by degradation of the perilipin protein: Nelfinavir enhances lysosome-mediated perilipin proteolysis. J Biol Chem. 2007
19. Nakagomi S, Suzuki Y, Namikawa K, Kiryu-Seo S, Kiyama H. Expression of the activating transcription factor 3 prevents c-Jun N-terminal kinase-induced neuronal death by promoting heat shock protein 27 expression and Akt activation. J Neurosci 2003;23:5187–96. [PubMed: 12832543]
20. Cadoudal T, Leroyer S, Reis AF, et al. Proposed involvement of adipocyte glyceroneogenesis and phosphoenolpyruvate carboxykinase in the metabolic syndrome. Biochimie 2005;87:27–32. [PubMed: 15733733]
21. Krueger SK, Williams DE. Mammalian flavin-containing monooxygenases: structure/function, genetic polymorphisms and role in drug metabolism. Pharmacology & therapeutics 2005;106:357–87. [PubMed: 15922018]
22. Zhou H, Gurley EC, Jarujaron S, et al. HIV protease inhibitors activate the unfolded protein response and disrupt lipid metabolism in primary hepatocytes. American journal of physiology 2006;291:G1071–80. [PubMed: 16861219]
23. Miura S, Gan JW, Brzostowski J, et al. Functional conservation for lipid storage droplet association among Perilipin, ADRP, and TIP47 (PAT)-related proteins in mammals, Drosophila, and Dictyostelium. J Biol Chem 2002;277:32253–7. [PubMed: 12077142]
24. Miyata Y, Fukuhara A, Matsuda M, Komuro R, Shimomura I. Insulin induces chaperone and CHOP gene expressions in adipocytes. Biochemical and biophysical research communications 2008;365:826–32. [PubMed: 18035047]

25. Ozcan, U.; Cao, Q.; Yilmaz, E., et al. Science. 306. New York, N.Y: 2004. Endoplasmic reticulum stress links obesity, insulin action, and type 2 diabetes; p. 457-61.
26. Waskiewicz AJ, Flynn A, Proud CG, Cooper JA. Mitogen-activated protein kinases activate the serine/threonine kinases Mnk1 and Mnk2. The EMBO journal 1997;16:1909–20. [PubMed: 9155017]
27. Winzen R, Kracht M, Ritter B, et al. The p38 MAP kinase pathway signals for cytokine-induced mRNA stabilization via MAP kinase-activated protein kinase 2 and an AU-rich region-targeted mechanism. The EMBO journal 1999;18:4969–80. [PubMed: 10487749]
28. Adams, JM.; Cory, S. Science. 281. New York, N.Y: 1998. The Bcl-2 protein family: arbiters of cell survival; p. 1322-6.
29. Chen C, Lu XH, Yan S, Chai H, Yao Q. HIV protease inhibitor ritonavir increases endothelial monolayer permeability. Biochemical and biophysical research communications 2005;335:874–82. [PubMed: 16105660]
30. Zhong DS, Lu XH, Conklin BS, et al. HIV protease inhibitor ritonavir induces cytotoxicity of human endothelial cells. Arterioscler Thromb Vasc Biol 2002;22:1560–6. [PubMed: 12377730]
31. Kim RJ, Wilson CG, Wabitsch M, Lazar MA, Steppan CM. HIV protease inhibitor-specific alterations in human adipocyte differentiation and metabolism. Obesity (Silver Spring, Md 2006;14:994–1002.
32. McCawley LJ, Matrisian LM. Matrix metalloproteinases: they're not just for matrix anymore! Current opinion in cell biology 2001;13:534–40. [PubMed: 11544020]
33. Clement K, Viguerie N, Poitou C, et al. Weight loss regulates inflammation-related genes in white adipose tissue of obese subjects. Faseb J 2004;18:1657–69. [PubMed: 15522911]
34. Westhoff, JH.; Sawitza, I.; Keski-Oja, J.; Gressner, AM.; Breitkopf, K. Growth factors. 21. Chur, Switzerland: 2003. PDGF-BB induces expression of LTBP-1 but not TGF-beta1 in a rat cirrhotic fat storing cell line; p. 121-30.
35. Mondal D, Larussa VF, Agrawal KC. Synergistic antiadipogenic effects of HIV type 1 protease inhibitors with tumor necrosis factor alpha: suppression of extracellular insulin action mediated by extracellular matrix-degrading proteases. AIDS research and human retroviruses 2001;17:1569–84. [PubMed: 11779345]
36. Inohara N, Koseki T, Chen S, Wu X, Nunez G. CIDE, a novel family of cell death activators with homology to the 45 kDa subunit of the DNA fragmentation factor. Embo J 1998;17:2526–33. [PubMed: 9564035]
37. Nordstrom EA, Ryden M, Backlund EC, et al. A human-specific role of cell death-inducing DFFA (DNA fragmentation factor-alpha)-like effector A (CIDEA) in adipocyte lipolysis and obesity. Diabetes 2005;54:1726–34. [PubMed: 15919794]
38. Zhou Z, Yon Toh S, Chen Z, et al. Cidea-deficient mice have lean phenotype and are resistant to obesity. Nat Genet 2003;35:49–56. [PubMed: 12910269]
39. Iwawaki T, Akai R, Kohno K, Miura M. A transgenic mouse model for monitoring endoplasmic reticulum stress. Nature medicine 2004;10:98–102.
40. Acosta-Alvear D, Zhou Y, Blais A, et al. XBP1 controls diverse cell type-and condition-specific transcriptional regulatory networks. Molecular cell 2007;27:53–66. [PubMed: 17612490]
41. Li C, Wong WH. Model-based analysis of oligonucleotide arrays: expression index computation and outlier detection. Proceedings of the National Academy of Sciences of the United States of America 2001;98:31–6. [PubMed: 11134512]
42. Pfaffl MW. A new mathematical model for relative quantification in real-time RT-PCR. Nucleic acids research 2001;29:e45. [PubMed: 11328886]

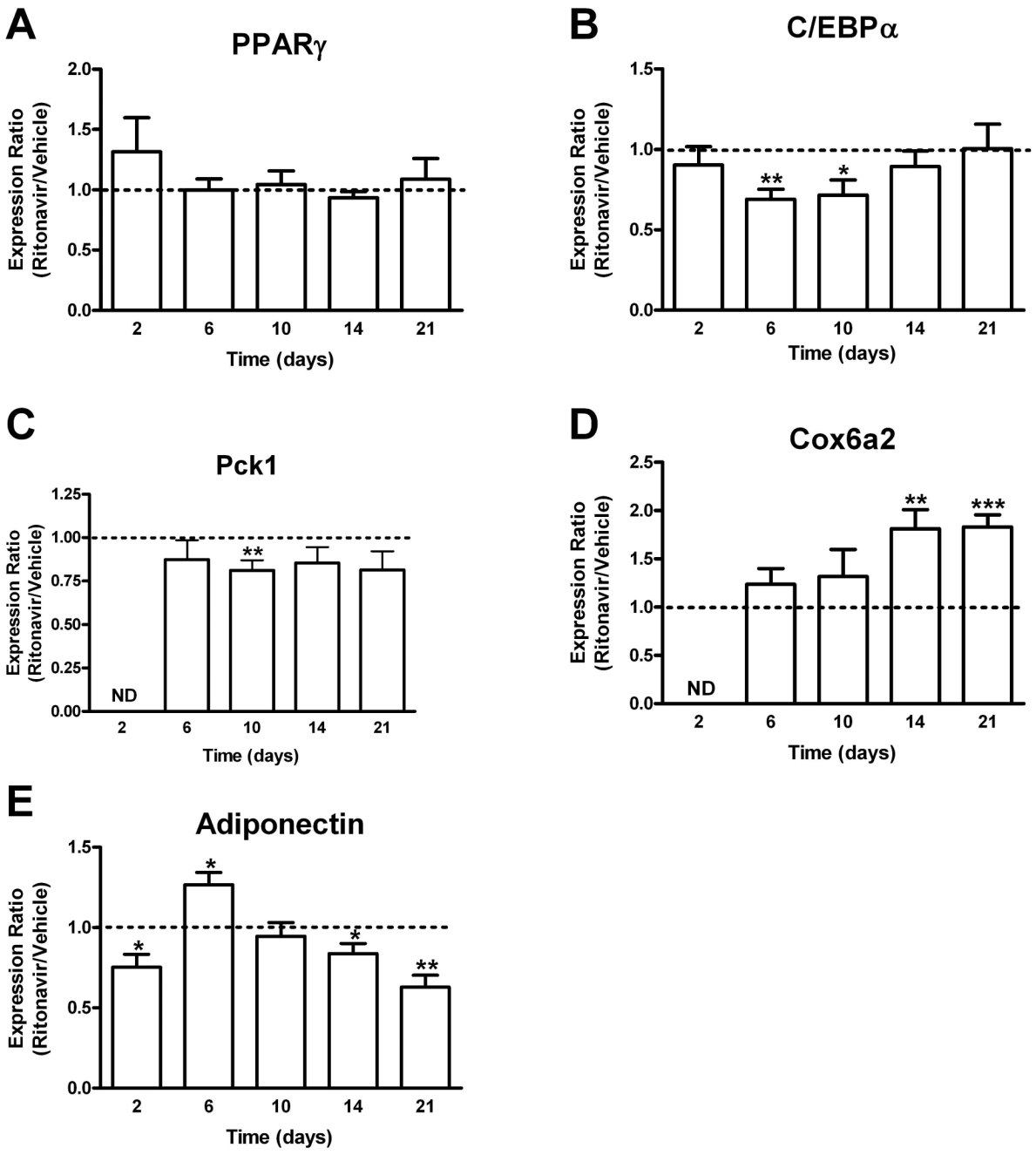

Figure 1.

Real Time PCR expression ratios showing changes in: (A) CCAAT/enhancer binding protein (C/EBPα), (B) peroxisome proliferator activated receptor gamma (PPARγ), (C) phosphoenolpyruvate carboxykinase 1 (Pck1), (D) cytochrome c oxidase, subunit VI a, polypeptide 2 (Cox6a2), and (E) adiponectin expression due to10 μM ritonavir treatment. Mean expression ratios for ritonavir- relative to vehicle-treated cells with SEM are reported (n=7-8) from 2 independent experiments. The dashed line indicates an expression ratio of 1.0, where the gene expression would be equivalent in ritonavir vs. vehicle. Mean ratios less than 1 suggest ritonavir treatment reduced expression, whereas mean ratios greater than 1 suggest ritonavir

treatment induced gene expression. *p<0.05, **p<0.01, and ***p<0.001, for mean expression ratio different from 1.0. ND; expression not detected.

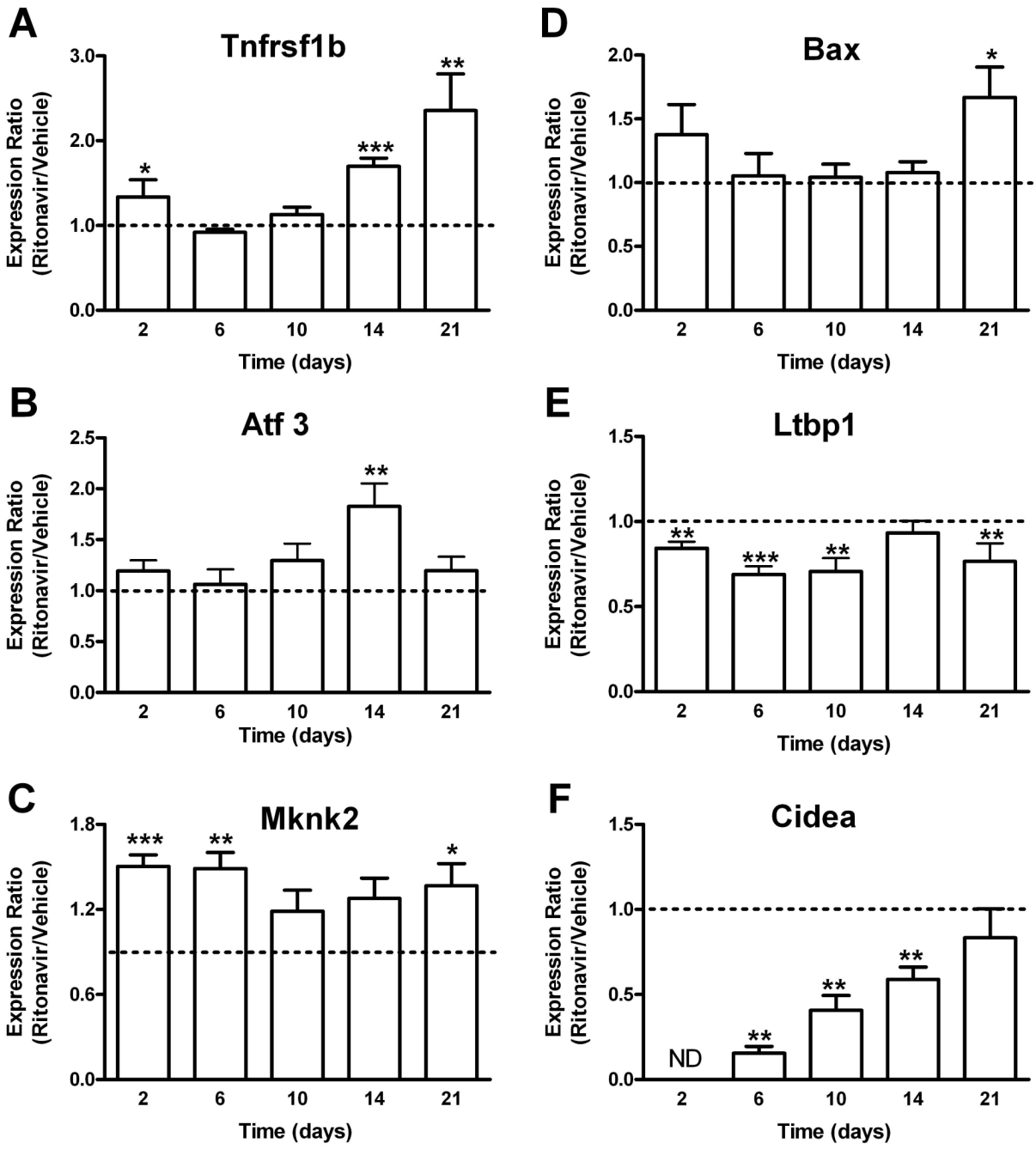

Figure 2.

Real Time PCR expression ratios showing changes in (A) tumor necrosis factor receptor superfamily, member 1b (Tnfrsf1b), (B) activating transcription factor 3 (Atf3), (C) MAP kinase-interacting serine/threonine kinase 2 (Mknk2), (D) Bcl2-associated X protein (Bax), (E) latent transforming growth factor beta binding protein 1 (Ltbp1), and (F) cell death-inducing DNA fragmentation factor, alpha subunit-like effector A (Cidea) expression due to 10 μM ritonavir treatment. Mean expression ratios with SEM are reported (n=6-8). See figure 1 for other details. $^{*}p<0.05$, $^{**}p<0.01$, and $^{***}p<0.001$ for mean expression ratio different from 1.0. ND; expression not detected.

Table 1

Effects of 10μM ritonavir on gene expression over time in 3T3-L1 adipocytes

Table 1A

Gen Bank Accession #	Gene Symbol	Gene Name (Categorized by Function)	Time (days post confluence)					p-value for Ritonavir (R) vs Vehicle (V) Overall
			2	6	10	14	21	
			Fold Change Gene Expression (R/V)					
		Differentiation						
U10374	PPAR-gamma	peroxisome proliferator activated receptor-gamma	-1.03	-1.15	-1.19	-1.18	-1.30	0.77
X66223	RXR-alpha	Retinoid X Receptor-alpha	1.05	1.42	1.16	1.24	-1.05	0.64
X57638	PPAR-alpha	peroxisome proliferator activated receptor-alpha	1.72	1.54	1.12	-2.35	1.15	0.054
X12761	c-jun	JUN oncogene	1.26	-6.46	-2.00	-10.08§	1.57	0.68
V00727	c-fos	FBJ osteosarcoma oncogene	1.41	1.32	2.47	1.83	3.73	0.21
L00039	c-myc	Myelocytomatosis oncogene	1.28	-1.18	1.64	1.40	2.22	0.23
X61800	C/EBP-delta	CCAAT/enhancer binding protein-delta	-1.07	-1.24	-1.43	-1.64	-1.42	0.58
M61007	C/EBP-Beta	CCAAT/enhancer binding protein-beta	1.14	-1.05	1.12	-1.11	1.39	0.66
M62362	C/EBP-alpha	CCAAT/enhancer binding protein-alpha	-1.01	1.35	1.05	-1.16	1.09	0.56
		Insulin Signaling						
X69722	IRS-1	Insulin Receptor Substrate-1	1.97	2.74	1.00	1.85	2.98	0.96
AF090738	IRS-2	Insulin Receptor Substrate-2	-1.08	1.54	1.53	1.44	2.71	0.76
AW121773	PI3K- p110α	Phosphatidylinositol 3-Kinase p110α subunit	-1.33	-1.20	-2.21	-1.00	1.20	0.18
U50413	PI3K- p85α	Phosphatidylinositol 3-Kinase p85α subunit	-1.48	1.53	1.29	1.11	1.66	0.21
AF079535	PDK1	3-phosphoinositide dependant protein kinase-1	-1.14	1.43	-1.02	-1.01	1.50	0.83
X65687	PKB/Akt1	thymoma viral proto-oncogene 1	1.16	1.09	1.11	1.12	1.52	0.97
AV367375	aPKC-ζ	atypical Protein Kinase C-ζ	-1.06	-1.57	22.66#	-1.89	1.45	0.33
L28035	aPKC-γ	atypical Protein Kinase C-γ	1.07	1.21	1.36	1.16	1.44	0.67
AI050321	Shc	src homology 2 domain-containing transforming protein C1	1.12	-1.18	1.13	1.07	1.49	0.64
U07617	Grb2	Growth factor receptor bound protein-2	1.26	-1.29	-1.13	-3.95	1.51	0.61
Z11574	SOS-1	Son of sevenless homolog 1	1.30	-1.59	-1.23	-1.10	1.10	0.84
Z11664	SOS-2	Son of sevenless homolog 2	1.23	-6.90	-1.27	-1.97	-1.78	0.63
Z50013	H-Ras	Harvey rat sarcoma virus oncogene	-1.20	-1.03	1.03	1.02	-1.05	0.90
M13071	Raf	Raf-related oncogene	-1.16	-1.23	1.35	1.37	-1.79	0.50
Z14249	ERK-1	extracellular-signal-regulated-kinase 1	1.23	1.30	1.05	1.16	1.06	0.96
		Lipid Metabolism						
AF009605	Pck1	phosphoenolpyruvate carboxykinase 1, cytosolic (glyceroneogenesis)	-1.56	-2.15	-1.68	-1.26	-1.67	0.0003
X99347	Lbp	lipopolysaccharide binding protein	-1.23	-8.42	-8.55	-24.74§	-8.86§	0.0195
AI846600	Mgll	EST AA589436 (cluster includes AI846600, monoglyceride lipase)	-1.36	1.44	-1.73	-2.55	-2.88	0.0103
X82648	Apod	apolipoprotein D	-1.64	1.19	-2.93	-1.24	-1.49	0.0040
D29016	Fdft1	farnesyl diphosphate farnesyl transferase 1	1.06	1.50	1.14	-1.03	1.11	0.0041
L02331	Sult1a1	sulfotransferase family 1A, phenol-preferring, member 1	-31.80§	1.15	-1.48	-1.73	-2.45	0.0000

Table 1B

Gen Bank Accession #	Gene Symbol	Gene Name (Categorized by Function)	Time (days post confluence)					p-value for Ritonavir (R) vs Vehicle (V) Overall
			2	6	10	14	21	
			Fold Change Gene Expression (R/V)					
		Mitochondrion/Endoplasmic Reticulum						
AV318575	FMO5	flavin containing monooxygenase 5	-1.48	-1.38	1.05	-1.15	-1.50	0.064
U08439	Cox6a2	cytochrome c oxidase, subunit VI a, polypeptide 2	-1.00	2.50	2.04	3.07	4.57	0.0005
D16215	FMO1	flavin containing monooxygenase 1	-1.30	-2.28	-1.53	-2.02	-2.08	0.0000

Table 1B

Gen Bank Accession #	Gene Symbol	Gene Name (Categorized by Function)	Time (days post confluence)					p-value for Ritonavir (R) vs Vehicle (V) Overall
			2	6	10	14	21	
			Fold Change Gene Expression (R/V)					
U29530	ATP-synt_B	ATP synthase, H+ transporting, mitochondrial F0 complex, subunit b, isoform	-1.48	-2.48	-1.10	-1.28	-2.24	0.10
		Transcription Factors/DNA binding						
Y11092	Mknk2	MAP kinase-interacting serine/threonine kinase 2	1.84	4.59	1.49	1.84	2.07	0.013
U19118	Atf3	activating transcription factor 3	1.38	-1.13	1.04	1.16	1.38	0.073
M94087	Atf4	activating transcription factor 4	1.44	1.48	1.38	1.57	1.29	0.0008
AI834866	Ncoa4	nuclear receptor coactivator 4	1.12	-1.20	-1.06	-1.43	-1.38	0.0046
AW123880	XBP-1	X-box binding protein 1	1.31	-1.41	-1.03	-1.32	-1.13	0.3595
X67083	CHOP-10	DNA-damage inducible transcript 3 (cluster includes CHOP-10)	1.18	1.10	-1.01	1.43	1.21	0.2252
X14678	TIS11	zinc finger protein 36/Mouse TPA-induced TIS11 mRNA	2.07	1.61	1.71	1.99	3.44	0.021
AJ237846	Rbmx	RNA binding motif protein, X chromosome	-1.51	-2.23	-1.64	-2.48	-2.81	0.0037
M28845	Krox-24	Mus musculus zinc finger protein (Krox-24) gene, exon 2	2.28	1.23	2.48	2.21	4.42	0.0043
AI846319	Rangnrf	RAN guanine nucleotide release factor	1.17	1.00	3.22	4.12	20.41	0.025
AF017806	Zfp-15	zinc finger protein 292/Mus musculus Zn-15 transcription factor	-2.01	-2.99	-1.95	-4.83	-1.43	0.027
AF017128	Fosl1	fos-like antigen 1	1.47	-1.39	1.72	1.41	5.42	0.0119
U20735	Junb	Jun-B oncogene	2.18	4.71	2.03	232.18#	61.71#	0.0001
AW047343	Dbp	D site albumin promoter binding protein (transcription factor)	-13.45	-2.03	-1.29	-1.47	-1.69	0.0007
		Apoptosis						
AF041376	Cidea	cell death-inducing DNA fragmentation factor, alpha subunit-like effector A	-4.31	-49.52§	-3.63	-1.95	-1.75	0.0093
L22472	Bax	Bcl2-associated X protein	1.14	1.69	1.14	2.40	1.20	0.0315
AF011908	Aatk	apoptosis-associated tyrosine kinase	1.05	-1.15	-1.37	-1.31	-1.53	0.0017
L28827	Hdh	Huntington disease gene homolog (anti-apoptosis)	1.01	1.57	1.15	1.01	-1.07	0.0022
AV298640	F7	coagulation factor VII	-1.08	50.66#	1.72	3.57	1.98	0.015
U63720	Casc3	caspase 3, apoptosis related cysteine protease	1.01	-1.01	1.13	-1.02	1.16	0.40
		Inflammation/Immune Response/Adipokines						
M63697	Cd1d1 /// Cd1d2	CD1d1 antigen	1.13	-1.01	-1.29	-1.20	-2.11	0.0006
M63695	Cd1d1	CD1d1 antigen	1.24	-1.43	-1.62	-1.80	-2.57	0.0007
M30136	Il9	interleukin 9	10.36	1.47	1.44	2.40	4.21	0.0480
X54542	Il6	Interleukin 6	1.19	-1.00	-4.30	-4.16	1.23	0.2173
AF022371	Ifi203	interferon activated gene 203	-6.27	-14.86§	-2.58	-1.28	1.04	0.0076
X69620	Inhbb	inhibin beta-B	-1.00	-4.07	-3.13	-2.91	-2.76	0.017
AV364086	Thbd	thrombomodulin	1.21	-1.15	-1.65	-1.94	-2.12	0.0081
D10214	Prlr	prolactin receptor	-1.76	1.23	-1.67	-2.32	-1.75	0.0008
D17433	Ptgfr	prostaglandin F receptor	1.08	-1.28	-1.14	-1.29	-1.40	0.0060
AI837679	Ormdl3	ORM1-like 3 (S. cerevisiae)/RIKEN cDNA 281001N17	1.00	1.03	1.00	-1.23	-1.23	0.0064
U49513	Ccl9	chemokine (C-C motif) ligand 9	1.00	1.91	3.08	3.00	2.22	0.0002
AI882416	Lep	leptin	-1.83	1.27	-1.10	-1.37	-1.49	0.2130
X57796	Tnfrsf1a	tumor necrosis factor receptor superfamily, member 1a	1.04	1.16	1.11	1.05	1.10	0.358
X87128	Tnfrsf1b	tumor necrosis factor receptor superfamily, member 1b (p75)	1.15	-1.11	1.07	1.30	1.77	0.0137
AI509617	Tnfaip1	tumor necrosis factor, alpha-induced protein 1 (endothelial)	1.22	-1.13	-1.31	1.10	1.72	0.80
L24118	Tnfaip2	tumor necrosis factor, alpha-induced protein 2	1.36	1.62	-2.40	1.40	2.04	0.70

Table 1C

Gen Bank Accession #	Gene Symbol	Gene Name (Categorized by Function)	Time (days post confluence)					p-value for Ritonavir (R) vs Vehicle (V) Overall
			2	6	10	14	21	
			Fold Change Gene Expression (R/V)					
		Extracellular matrix/Cell adhesion/Cytoskeletal						
U77630	Adm	adrenomedullin	-2.81	-14.69§	-1.79	-1.06	-1.40	0.037
AF022889	Ltbp1	latent transforming growth factor beta binding protein 1	-2.19	-6.98	-11.94	-1.72	-4.14	0.028
AW121179	Mfap5	microfibrillar associated protein 5 (extracellular matrix conferring	-1.19	-1.93	-1.29	-1.39	-1.81	0.0034
U43298	Lamb3	laminin, beta 3	-1.00	-10.52§	-3.21	-2.56	-5.19	0.0047
AV230686	Tnc	tenascin C	-1.70	-11.43§	-4.39	-3.30	-1.87	0.0020
AF013262	Lum	lumican	-1.59	-2.18	-2.04	-2.06	-2.18	0.0082
K03235	Plf	proliferin 2	1.91	-1.39	37.35#	13.09#	50.43#	0.016
X16009	Plf	mitogen regulated protein, proliferin 3	2.04	1.03	2.01	4.90	4.53	0.0004
D31951	Ogn	osteoglycin	-4.54	-2.80	-1.61	-1.57	-1.04	0.0027
AF078705	Vap-1	amine oxidase, copper containing 3/vascular adhesion protein-1	-2.08	1.04	-1.42	-1.50	-1.69	0.0299
U26437	Timp3	tissue inhibitor of metalloproteinase 3	1.04	-3.27	-1.69	-1.71	-1.20	0.0003
D38162	Col11a1	procollagen, type XI, alpha 1	-1.65	-1.49	-1.26	-1.69	-1.37	0.0001
L19932	Tgfbi	transforming growth factor, beta induced (cell adhesion)	1.41	-1.23	-1.88	-1.82	-1.23	0.019
AA717826	Dpt	dermatopontin (cell matrix, cell adhesion)	-1.17	-2.11	-2.39	-2.73	-1.86	0.0001
X69902	Itga6	integrin alpha 6 (cell adhesion)	-1.29	-1.59	-1.20	-1.87	-1.19	0.0002
AA647799	Ogn	osteoglycin	-79.88§	-17.90§	-1.69	-2.51	-1.72	0.0004
D31951	Ogn	osteoglycin	-4.54	-2.80	-1.61	-1.57	-1.04	0.0027

Fold changes in gene expression due to ritonavir treatment are reported for each time point and sorted by function. Changes in gene expression due to treatment across time were considered significantly different at $p<0.05$.

The calculated fold changes were unusually large for some genes due to low expression in either vehicle or ritonavir

§ treated cells.